



Comparative analysis of larval growth in Lepidoptera reveals instar-level constraints

Sami M. Kivelä¹  | Robert B. Davis¹ | Toomas Esperk¹ | Karl Gotthard² | Marko Mutanen³ | Daniel Valdma¹ | Toomas Tammaru¹ 

¹Department of Zoology, Institute of Ecology and Earth Sciences, University of Tartu, Tartu, Estonia

²Department of Zoology, Stockholm University, Stockholm, Sweden

³Department of Ecology and Genetics, University of Oulu, Oulu, Finland

Correspondence

Sami M. Kivelä
Email: sami.kivela@oulu.fi

Present address

Sami M. Kivelä, Department of Ecology and Genetics, University of Oulu, PO Box 3000, FI-90014, Oulu, Finland

Funding information

Emil Aaltosen Säätiö; Estonian Ministry of Education and Research, Grant/Award Number: IUT20-33; Eesti Teadusagentuur, Grant/Award Number: PUT1474; Biotieteiden ja Ympäristön Tutkimuksen Toimikunta, Grant/Award Number: 277984, 314833 and 319898; Vetenskapsrådet, Grant/Award Number: VR 2017-04500; Suomen Kulttuurirahasto; Bolin Centre for Climate Research at Stockholm University; Stockholm University; Finnish Cultural Foundation

Handling Editor: Johannes Overgaard

Abstract

1. Juvenile growth trajectories evolve via the interplay of selective pressures on age and size at maturity, and developmental constraints. In insects, the moulting cycle is a major constraint on larval growth trajectories.
2. Surface area to volume ratio of a larva decreases during growth, so renewal of certain surfaces by moulting is likely needed for the maintenance of physiological efficiency. A null hypothesis of isometry, implied by Dyar's Rule, would mean that the relative measures of growth remain constant across moults and instars.
3. We studied ontogenetic changes and allometry in instar-specific characteristics of larval growth in 30 lepidopteran species in a phylogenetic comparative framework.
4. Relative instar-specific mass increments (RMI) typically, but not invariably, decreased across instars. Ontogenetic change in RMIs varied among families with little within-family variation. End-of-instar growth deceleration (GD) became stronger with increasing body size across instars. Across-instar change in GD was conserved across taxa. Ontogenetic allometry was generally non-isometric in both RMI and GD.
5. Results indicate that detailed studies on multiple species are needed for generalizations concerning growth trajectory evolution. Developmental and physiological mechanisms affecting growth trajectory evolution show different degrees of evolutionary conservatism, which must be incorporated into models of age and size at maturation.

KEYWORDS

allometry, cutaneous respiration, moulting, oxygen limitation, phylogenetic comparative methods, relative mass increment

1 | INTRODUCTION

Understanding developmental and physiological mechanisms that generate evolutionary constraints is vital in evolutionary biology

(Davidowitz, Roff, & Nijhout, 2016; Nijhout, Roff, & Davidowitz, 2010; Roff, 2002; Stearns, 1992; see also Gould & Lewontin, 1979, and contributions in Flatt & Heyland, 2011). Constraints either slow down the rate of phenotypic evolution or render some phenotypes

This is an open access article under the terms of the Creative Commons Attribution License, which permits use, distribution and reproduction in any medium, provided the original work is properly cited.

© 2020 The Authors. *Functional Ecology* published by John Wiley & Sons Ltd on behalf of British Ecological Society

completely impossible (Roff & Fairbairn, 2007). As a result, trait values may not reach optima that would be expected on the grounds of ecologically based selection pressures. For example, it has been argued that viviparity would be optimal for birds under certain conditions, but it has never evolved in birds due to physiological constraints (Blackburn & Evans, 1986; Dunbrack & Ramsay, 1989). In phylogenetic, among-species comparisons, constraints become apparent as conservatism of trait values (see Schwenk & Wagner, 2004; Tammaru, Esperk, Ivanov, & Teder, 2010; Tammaru, Vellau, Esperk, & Teder, 2015), yet conservatism may also result from strong and consistent stabilizing selection acting on a clade.

Age and size at maturity are central life-history traits that are, perhaps universally, under strong ecological selection (Roff, 2002; Stearns, 1992). Yet, juvenile growth trajectories—the proximate determinants of age and size at maturity—are shaped by developmental and physiological mechanisms that may act as evolutionary constraints. Hence, conservative elements of juvenile growth trajectories identified by phylogenetic comparative analyses could reveal constraints on age and size at maturity.

Insects have become a model system for studying growth and associated developmental and physiological mechanisms (Callier & Nijhout, 2013; Gokhale & Shingleton, 2015; Nijhout, Davidowitz, & Roff, 2006; Nijhout et al., 2010, 2014; Shingleton, 2011) and their life-history implications (Davidowitz et al., 2016; Hironaka & Morishita, 2017; Kivelä, Friberg, Wiklund, Leimar, & Gotthard, 2016). However, research has focused on just a few model species. As a consequence, the missing comparative perspective precludes generalizations about potential constraints on insect growth trajectory evolution.

In insects, ontogenetic growth is restricted to the larval stage, and regular replacement of the exoskeleton in a process called moulting makes the growth trajectory discontinuous. Body mass increases between the moults (i.e. during a larval instar), whereas the dimensions of the strongly sclerotized (i.e. inextensible) parts of the exoskeleton only increase at moults (Chapman, 1998). The number of moults and the size increment of each instar determine the peak mass of the larva, and thereby, largely, the size of an insect at maturity. Age at maturity is directly affected by the number of moults because physiological preparation for moulting and the moulting process itself take time; across all moults, this time forms a considerable part of the duration of the larval stage. Therefore, the time taken to complete a moult and the number of instars have a major influence on the minimum possible age at maturity. Developmental and physiological mechanisms associated with the moulting process have, thus, the potential to act as important constraints on insect life-history evolution (Davidowitz et al., 2016; Nijhout et al., 2006, 2010; Tammaru, 1998; Tammaru et al., 2010, 2015).

The insect moulting cycle appears to be conservative both within and among species. The number of larval instars is usually invariant within a species (Esperk, Tammaru, & Nylin, 2007; Esperk, Tammaru, Nylin, & Teder, 2007), but varies between insect species (Chapman, 1998; Esperk, Tammaru, & Nylin, 2007; Esperk, Tammaru, Nylin, et al., 2007). However, in some species, the number of instars is sexually

dimorphic (Esperk, Tammaru, Nylin, et al., 2007), or it may vary in response to various environmental factors so that larvae growing under poor conditions add instars to reach a size threshold for a successful metamorphosis (Esperk, Tammaru, & Nylin, 2007; Greenberg & Ar, 1996; Grunert, Clarke, Ahuja, Eswaran, & Nijhout, 2015). Within-instar growth patterns also appear relatively conservative as divergent selection on adult body size may only slightly change relative size increments in any particular instar (Esperk, Tammaru, Nylin, et al., 2007; Meister, Hämäläinen, Valdma, Martverk, & Tammaru, 2018). Moreover, the relative size increment often remains constant across larval instars, which is an empirically broadly supported pattern known as Dyar's Rule (Berg & Merritt, 2009; Dyar, 1890; Hutchinson, McNamara, Houston, & Vollrath, 1997). However, there are deviations from the rule (Hutchinson et al., 1997; Kivelä, Friberg, et al., 2016; Meister et al., 2018), so quantification of conservative instar-level patterns in insect growth, as well as deviations from such patterns, may allow the identification of evolutionary constraints, which is needed for advancing our understanding of life-history evolution.

The key to locating instar-level constraints on larval growth in insects is in identifying the reasons for the moulting process itself. Ultimately, it is evident that an organism with an exoskeleton cannot grow indefinitely without moulting. However, it appears that moulting occurs before the theoretical instar growth limit is reached (cf. Kamimura & Kiuchi, 1998; Nijhout et al., 2006). Most hypotheses concerning moulting are related to allometry. Surface area to volume ratio inevitably changes with the growth of the organism, so various surfaces need to be periodically renewed to maintain physiological efficiency and functionality. Growth efficiency may decrease during an instar because of hypoallometric growth of the midgut (Esperk & Tammaru, 2004; Grunert et al., 2015), a fixed sized or hypoallometrically growing tracheal respiratory system (Callier & Nijhout, 2011; Greenberg & Ar, 1996; Greenlee & Harrison, 2004, 2005), fixed-sized structures used in food acquisition (Hutchinson et al., 1997), or because of the restricted capacity of the cuticle to expand (Bennet-Clark, 1963). Owing to allometry, the extent to which the area of a surface becomes limiting depends on the absolute size of the larva (cf. Kühnel, Brückner, Schmelzle, Heethoff, & Blüthgen, 2017). As these patterns are based on fundamental physical principles, we would expect a high degree of similarity in these relationships across species and instars.

To test the null hypothesis of isometry (i.e. Dyar's Rule; invariance of relative growth patterns across instars), we recorded two key parameters of larval growth trajectories—instar-specific relative mass increments (RMI) and end-of-instar growth deceleration (GD; Figure 1)—from 30 species of Lepidoptera. Our analysis identifies deviations from isometry in the measured traits. We proceed by evaluating phylogenetic conservatism of the examined traits, with the aim to quantify the degree to which these traits may constrain adaptive evolution of age and size at maturity. Finally, we discuss the data in the light of different hypotheses proposed to explain the ultimate causes and proximate triggers of the moulting process.

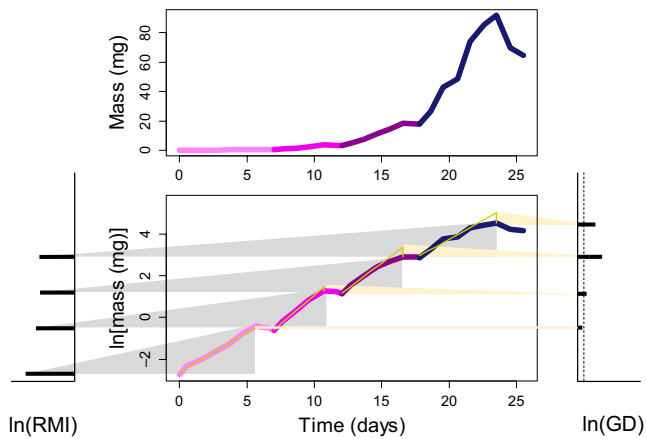


FIGURE 1 Illustration of an insect larval growth trajectory describing how relative instar-specific mass increment (RMI) and end-of-instar growth deceleration (GD) are estimated. Top panel shows the growth trajectory of an individual *Xanthorhoe fluctuata* (Lepidoptera: Geometridae) larva chosen arbitrarily for illustrative purposes. The four larval instars are indicated with different colours. The bottom-centre panel shows the same growth trajectory with ln-transformed mass, clearly visualizing moults and associated mass loss. The grey triangles project the differences (in ln-scale) between instar-specific peak mass and initial mass to the bar plot on the left. Each horizontal bar represents the difference between instar-specific ln[peak mass] and ln[initial mass], which is equal to ln[RMI] (i.e. $RMI = [\text{instar peak mass}] / [\text{instar initial mass}] = \exp(\ln[\text{instar peak mass}] - \ln[\text{instar initial mass}])$). The yellow lines overlaying instar-specific growth trajectories are fitted regressions for instar-specific data, but with the latter part of the instar-specific growth trajectory excluded from regression analysis (see text and Figure S2 for details). Consequently, the regression lines extrapolate growth in the latter part of each instar as if growth continued exponentially until the end of the instar. The difference between extrapolated instar-specific peak mass and the observed instar-specific peak mass is illustrated by the vertical yellow lines. These differences are equal to ln(GD) (i.e. $GD = [\text{extrapolated instar peak mass}] / [\text{observed instar peak mass}] = \exp(\ln[\text{extrapolated instar peak mass}] - \ln[\text{observed instar peak mass}])$). The yellow triangles project instar-specific GD values to the bar plot on the right (the bars have been scaled up to make reading easier), the horizontal bars illustrating instar-specific values of GD. The vertical dashed line in the right panel indicates zero (corresponds to one in the arithmetic scale), below which growth in fact accelerates towards the end of an instar, which is the case in the first instar in this example

2 | MATERIALS AND METHODS

2.1 | Growth trajectory data acquisition

We obtained detailed growth trajectory data from 30 lepidopteran species from 11 families (Table 1). We used earlier-published data on five species (Leimar, 1996; Esperk et al., 2013; Kivelä, Friberg, Wiklund, Leimar, & Gotthard, 2015; see Table 1), but most of the data were collected specifically for the purposes of the present study. Butterflies and moths were captured in Oulu (Finland), Tartu County (Estonia) and Stockholm (Sweden). Captured females were

allowed to oviposit on natural host plants in the laboratory (see Table 1 for the host plants used). Neonate larvae were weighed and individually placed in plastic containers with ad libitum natural host plant. A split-brood design was used for larvae reared at the University of Tartu, with broods being split between 16 and 24°C constant temperatures (day length 12 hr) whenever possible (see Table 1). Larvae reared at the University of Oulu experienced a day length of 16 hr and an associated thermal cycle between 18°C (photophase) and 10°C (scotophase). At Stockholm University, extra *Pieris napi* larvae, in addition to those included in the previously published dataset (Kivelä et al., 2015), were reared at a constant 16°C under a 17 hr day length. All larvae were weighed one to three times per day until pupation, depending on temperature; weighing was more frequent at higher temperatures. Moulting events were recorded both by direct observations and indirectly from recording the growth trajectory (larvae lose mass during moulting; see below for details). Sphingids were not weighed or handled during moulting because handling at this stage may easily be fatal for these species. Once the pupal moult was completed and the pupal cuticle had hardened, pupal mass was measured and sex was determined based on genital slits in the pupal cuticle. We combined all the datasets to test whether the analysed traits depend on temperature.

2.2 | Analysed traits

We focused on relative instar-specific mass increments (RMI) and end-of-instar GD. We calculated RMI as the ratio of the peak mass of the focal instar to the initial mass of the same instar. For quantification of GD, we used a modification of the approach used by Esperk and Tammaru (2004) in which GD is estimated by comparing the instar-specific peak mass that would have been attained without GD and the peak mass of the instar actually attained. We extrapolated growth until the time point where mass accumulation ceases in the focal instar by assuming exponential growth instead of the allometric power 2/3 relationship used by Esperk and Tammaru (2004). Then, we calculated the ratio of extrapolated instar-specific peak mass to the observed instar-specific peak mass (see below for details). A higher ratio indicates a stronger deceleration of growth at the end of the instar.

Next, we quantified ontogenetic change in RMIs and GD as regression slopes capturing across-instar changes in the instar-specific characteristics. Ontogenetic change in RMIs was analysed by fitting a linear regression model of ln-transformed RMI values on ln-transformed instar-specific initial masses separately for each individual (Figure S1). Logarithmic transformations were used to linearize the relationship between the traits and also because this is conventional in analyses of allometric scaling of trait values to body size (see e.g. Kilmer & Rodríguez, 2017). The slopes of these RMI regressions (hereafter the relative mass increment slope, RMIS) capture ontogenetic across-instar change (or lack of it) in the relative amount of growth within an instar.

TABLE 1 List of species included in the experiment. Sample sizes, host plants and rearing temperatures are indicated as well as median number of larval instars (and range, if the number of instars varied), neonate larval mass and peak larval mass; standard error included for the latter two traits

Species	Family	N ^a	Sampling location	Host plant	Rearing temperature (°C)	Day length (hr)	Median (range) ^b number of larval instars	Mean neonate larval mass (mg) (SE) ^c	Mean peak larval mass (mg) (SE) ^c
<i>Achlya flavicornis</i> ^d	Drepanidae	2	Oulu, Finland	<i>Betula pubescens</i>	18/10 cycle ⁱ	16	5	0.180 (0.0300)	719 (30.4)
<i>Drepana falcataria</i> ^e	Drepanidae	36	Tartu county, Estonia	<i>Betula pendula</i>	16; 24	12	4	0.123 (0.00335)	129 (4.01)
<i>Falcaria lacertinaria</i> ^e	Drepanidae	13	Tartu county, Estonia	<i>Betula pendula</i>	24	12	4 (4–5)	0.158 (0.0140)	138 (4.10)
<i>Endromis versicolora</i> ^d	Endromidae	3	Oulu, Finland	<i>Betula pendula</i>	18/10 cycle ⁱ	16	5	2.42 (0.0252)	2,824 (292)
<i>Scoliopteryx libatrix</i> ^d	Erebidae	5	Oulu, Finland	<i>Salix phylicifolia</i>	18/10 cycle ⁱ	16	5	0.150 (0.00707)	500 (11.3)
<i>Spilosoma lubricipedum</i> ^e	Erebidae	19	Tartu county, Estonia	<i>Urtica dioica</i>	16; 24	12	7 (6–8)	0.245 (0.0170)	704 (23.7)
<i>Biston betularia</i> ^e	Geometridae	8	Tartu county, Estonia	<i>Betula pendula</i>	8	12	5 (5–6)	0.0974 (0.00192)	707 (34.1)
<i>Calospilos sylvata</i> ^e	Geometridae	24	Tartu county, Estonia	<i>Prunus padus</i>	16; 24	12	5 (5–6)	0.102 (0.00307)	122 (3.79)
<i>Eupithecia subfuscata</i> ^e	Geometridae	1	Tartu county, Estonia	<i>Alnus incana</i>	16	12	4	0.0360 (–)	15.1 (–)
<i>Paradarisa consonaria</i> ^e	Geometridae	19	Tartu county, Estonia	<i>Betula pendula</i>	16; 24	12	5 (5–6)	0.0658 (0.00120)	130 (2.77)
<i>Xanthorhoe fluctuata</i> ^e	Geometridae	12	Tartu county, Estonia	<i>Raphanus raphanistrum</i>	16; 24	12	4	0.0659 (0.00249)	73.7 (3.12)
<i>Polyommatus icarus</i> ^h	Lycaenidae	1	Öland, Sweden	<i>Medicago sativa</i>	23	19	4	0.0517 (0.00448)	95.7 (3.52)
<i>Brachionycha nubeculosa</i> ^e	Noctuidae	23	Tartu county, Estonia	<i>Prunus padus</i>	16; 24	12	6	0.352 (0.0178)	1774 (31.8)
<i>Conistra rubiginata</i> ^e	Noctuidae	21	Tartu county, Estonia	<i>Salix caprea</i>	16; 24	12	5 (5–6)	0.203 (0.00319)	485 (9.89)
<i>Conistra vaccini</i> ^e	Noctuidae	13	Tartu county, Estonia	<i>Prunus padus</i>	16; 24	12	6	0.146 (0.00836)	412 (16.0)
<i>Eupsilia transversa</i> ^e	Noctuidae	22	Tartu county, Estonia	<i>Prunus padus</i>	16; 24	12	6	0.0834 (0.00230)	723 (6.85)
<i>Orthosia gothica</i> ^d	Noctuidae	10	Oulu, Finland	<i>Prunus padus</i>	18/10 cycle ⁱ	16	6	0.113 (0.00667)	463 (8.44)
<i>Orthosia incerta</i> ^g	Noctuidae	21	Tartu county, Estonia	<i>Betula pendula</i> , <i>Prunus padus</i>	16; 18/10 cycle ⁱ ; 24	12	6 (6–7)	0.121 (0.00535)	665 (12.7)
<i>Trachea atriplicis</i> ^e	Noctuidae	3	Tartu county, Estonia	<i>Persicaria lapathifolia</i>	24	12	6	0.0963 (0.00120)	1716 (159)
<i>Cerura vinula</i> ^d	Notodontidae	3	Oulu, Finland	<i>Salix phylicifolia</i>	18/10 cycle ⁱ	16	5	1.74 (0.00882)	2,504 (157)
<i>Notodonta torva</i> ^e	Notodontidae	2	Tartu county, Estonia	<i>Populus tremula</i>	24	12	5	0.404 (0.000500)	819 (8.95)
<i>Pararge aegeria</i> ^h	Nymphalidae	2	Madeira, Portugal	<i>Dactylis glomerata</i>	18	15	4	0.290 (0.0156)	191 (8.53)
<i>Pararge xiphia</i> ^h	Nymphalidae	7	Madeira, Portugal	<i>Dactylis glomerata</i>	18	15	4	0.833 (0.0605)	404 (21.5)
<i>Iphiclides feisthamei</i> ^l	Papilionidae	78	Catalonia, region, Spain	<i>Prunus cerasifera</i>	22	12	5	–	1,069 (20.0)
<i>Gonepteryx rhamni</i> ^e	Pieridae	12	Tartu county, Estonia	<i>Frangula alnus</i>	16; 24	12	5	0.118 (0.00887)	380 (8.56)
<i>Pieris brassicae</i> ^e	Pieridae	6	Tartu county, Estonia	<i>Raphanus raphanistrum</i>	24	12	5	0.159 (0.0138)	583 (9.09)
<i>Pieris napi</i> ^{l,h}	Pieridae	32	Oulu, Finland; Stockholm, Sweden	<i>Alliaria petiolata</i>	16; 24	17	5	0.116 (0.00223)	184 (3.60)

(Continues)

TABLE 1 (Continued)

Species	Family	N ^a	Sampling location	Host plant	Rearing temperature (°C)	Day length (hr)	Median (range) ^b number of larval instars	Mean neonate larval mass (mg) (SE) ^c	Mean peak larval mass (mg) (SE) ^c
<i>Delilephila elpenor</i> ^e	Sphingidae	10	Tartu county, Estonia	<i>Epilobium angustifolium</i>	16; 24	12	5	2.12 (0.368)	5.932 (151)
<i>Laotioe populif</i> ^e	Sphingidae	11	Tartu county, Estonia	<i>Populus tremula</i>	16; 24	12	4 (4–5)	3.42 (0.0483)	2.463 (151)
<i>Smerinthus ocellatus</i> ^e	Sphingidae	6	Tartu county, Estonia	<i>Populus tremula</i>	24	12	6	1.63 (0.0459)	2,726 (181)

^aNumber of individuals included in the statistical analyses (i.e. the number of individuals with unambiguous data from ≥ 3 instars).

^bRange of larval instars observed in the experiment is indicated for those species that varied in the number of larval instars.

^cStandard error of the mean.

^dLarvae reared at University of Oulu, Finland.

^eLarvae reared at University of Tartu, Estonia.

^fLarvae reared at Stockholm University, Sweden.

^gSome larvae reared at University of Oulu, Finland, and some at University of Tartu, Estonia.

^hData published in Kivelä et al. (2015); *P. icarus* data originally from Leimar (1996).

ⁱTemperature was 18°C in the daytime and 10°C at night (i.e. thermoperiod of 16 hr 18°C:8 hr 10°C).

For GD, we tested the robustness of the results to the definition of the exponential growth phase at the beginning of the instar. For this purpose, we alternatively used the first 40%, 50%, 60%, 70% or 80% of within-instar mass measurements (rounded to an integer number of observations) from the growth phase of the instar (i.e. pre-moult mass loss was excluded) to describe exponential growth. A regression model was then used to estimate the hypothetical peak mass of the focal instar that would be attained if the exponential growth characteristic of the phase of 'free' growth (Grunert et al., 2015; Kivelä, Friberg, et al., 2016; Nijhout et al., 2006; Tammaru & Esperk, 2007) could be maintained through the instar (Figure S2). We repeated this procedure for each instar of each individual to derive instar- and individual-specific GD indices (i.e. $GD = [\text{instar peak mass based on extrapolating exponential growth}] / [\text{observed instar peak mass}]$). Then, to analyse ontogenetic change in GD, we fitted a regression of \ln -transformed GD values on \ln -transformed instar-specific peak masses for each individual. Instead of instar initial mass, instar peak mass is an appropriate independent variable for allometric analysis here because it closely correlates with the body size at which GD takes place. The slopes of these regressions (hereafter the growth deceleration slope, GDS) capture ontogenetic across-instar change (or lack of it) in GD. We repeated the derivation of individual-specific GDS values using the five alternative data-inclusion thresholds (40%, 50%, 60%, 70% and 80%) when extrapolating exponential growth for GD calculation. We present only results derived with the 70% threshold in the main text, whereas the results derived with the other thresholds are presented in Appendix A in Supporting Information. This is because low thresholds (40% and 50%) cause a lot of noise in the data due to uncertainty of the regression used in GD derivation, and 60% and 80% thresholds resulted in analytical problems (non-converging models and unrealistic estimates of phylogenetic signal; see Appendix A in Supporting Information).

Because both RMI and GD were quantified as ratios of masses and we use body mass as a measure of body size, the null hypothesis of isometry would mean constancy of RMI and GD across instars. Therefore, the isometric scaling exponent (i.e. value of RMIS or GDS) would be zero for both traits, if larvae grew isometrically.

We had to omit some instars of some individuals because moulting events could not always be unambiguously identified (7.2% of instars completed by the studied individuals). This is because, at high temperatures, some individuals moulted so rapidly that the actual moulting process could not be observed. Occasionally, moult-associated loss of mass (larvae cannot feed some time before and during moulting) could not be identified in the growth trajectory either. Therefore, we only analysed individuals from which the beginning and the end of a minimum of three instars could be unambiguously determined.

2.3 | DNA extraction and sequencing

To facilitate phylogenetic comparative analyses, DNA was extracted and sequenced for all 30 study species and used to infer phylogenetic relationships among them. To increase reliability of

the phylogeny, the sampling was supplemented with 10 additional closely related species (Table S1). These 10 species were pruned from the final phylogenetic tree used for subsequent analyses. Various body parts were used for DNA extraction, depending on a sample's life-history stage and size. DNA was extracted and purified using Qiagen's DNeasy Blood & Tissue extraction kit. DNA amplification and sequencing were predominantly carried out following standard protocols as explained in detail in Wahlberg and Wheat (2008), except for PCR clean-up that was carried out with ExoSAP-IT (Affymetrix) and Sephadex columns (Sigma-Aldrich), and sequencing that was done using an ABI 3730 DNA Analyzer (Applied Biosystems). Sanger sequencing was performed for one mitochondrial and seven nuclear markers: cytochrome oxidase subunit 1 gene (COI), carbamoylphosphate synthase domain protein (CAD), elongation factor 1 alpha (EF1a), glyceraldehyde-3-phosphate dehydrogenase (GAPDH), isocitrate dehydrogenase (IDH), cytosolic malate dehydrogenase (MDH), ribosomal protein S5 (RpS5) and wingless. The hybrid primers used are available at <http://www.nymphalidae.net/Molecular.htm>. This set of markers has proven to be efficient in Lepidoptera phylogenetics (Mutanen, Wahlberg, & Kaila, 2010) and has also been used in many studies focusing on the taxa included in this study (e.g. Heikkilä, Kaila, Mutanen, Pena, & Wahlberg, 2012; Sihvonen et al., 2011; Zahiri et al., 2010). Altogether, the gene regions used comprised a total of 6,286 base pairs. All sequences for each taxon were manually aligned and edited using BioEdit (Hall, 1999). All DNA sequences are available at the US National Center for Biotechnology Information (NCBI) GenBank (accessions numbers given in Table S2).

2.4 | Phylogeny derivation

An ultrametric phylogenetic tree based on the combined genes dataset was inferred using Bayesian inference (BI) through the CIPRES Science Gateway (Miller, Pfeiffer, & Schwartz, 2010). The

BI analysis was run in BEAST 1.8.0 (Drummond & Rambaut, 2007). The GTR + I + G substitution model was chosen according to the Akaike information criterion (AIC) value obtained in JMODELTEST 2.1.3 (Darriba, Taboada, Doallo, & Posada, 2012).

Base frequencies were estimated, the number of gamma categories was set to six and a randomly generated initial tree was used. A lognormal relaxed clock was employed and the tree prior was set to speciation: Yule Process. Parameters were estimated using two independent runs of 50 million generations each, and convergence was checked using the program TRACER 1.6 (Rambaut, Suchard, Xie, & Drummond, 2014). The derived phylogeny is archived in the Dryad Digital Repository (<https://doi.org/10.5061/dryad.p2ngf1vmz>; Kivelä et al., 2020).

2.5 | Statistical analyses

To analyse among-species variation in RMIS and GDS, we calculated species-specific means from individual-specific values of both RMIS and GDS, and analysed variation in species-specific trait values with the phylogenetic generalized least squares (PGLS) approach. We used R version 3.4.3 (R Core Team, 2017) for all the analyses. We calculated species-specific averages of RMIS and GDS across temperatures to take natural plasticity in growth trajectories into account (Table 2). We analysed temperature effects on RMIS and GDS with linear mixed-effect models (R function 'lme' from package NLME; Pinheiro, Bates, DebRoy, Sarkar, & R Core Team, 2017) by setting temperature as a fixed effect and species as a random effect. Temperature was nested within species to add power to the estimation of temperature effects. The PGLS analyses described later were conducted by both including and excluding the final larval instar. This robustness check was performed due to the physiological differences between the final instar and earlier ones (see e.g. Callier & Nijhout, 2013; Nijhout et al., 2014; Shingleton, 2011).

Trait	Parameter	Estimate	SE	df	t Value	p Value
RMIS ^a	Intercept (16°C)	-0.0666	0.0155	303	-4.29	<0.0001
	18°C	0.0605	0.0558	26	1.09	0.29
	18°C/10°C cycle	-0.0251	0.0200	13	-1.25	0.23
	23°C	0.0675	0.0865	26	0.780	0.44
	24°C	0.0245	0.00738	13	3.31	0.0056
GDS	Intercept (16°C)	0.0547	0.00734	380	7.45	<0.0001
	18°C	0.0818	0.0255	26	3.21	0.0035
	18°C/10°C cycle	-0.0184	0.0151	13	-1.22	0.24
	22°C	0.00683	0.0209	26	0.326	0.75
	23°C	0.0289	0.0621	26	0.465	0.65
	24°C	0.00873	0.00722	13	1.21	0.25

TABLE 2 Parameter estimates of (non-phylogenetic) linear mixed-effects models for analysing variation in RMIS and GDS in relation to temperature. Species was set as a random effect in these models as several individuals per species were included in the analysis, data coming from more than one rearing temperature for some species (see Table 1). The factor 'temperature' was nested within species

Abbreviations: GDS, growth deceleration slope; RMIS, relative mass increment slope.

^aThe model included an exponential variance function ('varExp'; Pinheiro et al., 2017) to take increasing residual variance with increasing fitted value into account.

In a PGLS framework, we first analysed the relationship between RMIS (response) and neonate larval mass (predictor; ln-transformed). For this, we used the functions 'gls' (package *NLME*; Pinheiro et al., 2017) and 'corPagel' (package *APE*; Paradis, Claude, & Strimmer, 2004), the latter of which first estimates (via maximum likelihood) the value of λ (i.e. phylogenetic signal) and then automatically applies the λ value in modelling correlations among residuals, thereby accounting for any phylogenetic non-independence of the observations. Neonate larval mass was set as a predictor because it captures variation in surface area to volume (A:V) ratio in first-instar larvae (high A:V ratio in small larvae), with this initial A:V ratio being potentially important to physiological functions affecting RMIS. Residual variance was much lower in butterflies (Lycaenidae, Nymphalidae and Pieridae; note that *Iphiclydes feisthamelii* [Papilionidae] was not included in this analysis due to missing data on neonate larval mass) than in moths (all other families represented in this study). The division between butterflies and moths represents the deepest phylogenetic split in our sample of species (note that this division is not the case in Lepidoptera as a whole—butterflies nest within moths [Mutanen et al., 2010]). The phylogenetic independence of these lineages in our sample (Figure S3; see also Figure S4) allowed us to model residual variance separately for butterflies and moths by adding a 'varIdent' variance function (Pinheiro et al., 2017) with 'major group' (butterfly/moth) as a variance covariate to the model. The model with the variance function was better than the one without it ($\Delta\text{AICc} = 6.73$).

Because initial investigation of the raw data indicated variation among taxonomic families (Figure S5), we continued by quantifying family-level variation in RMIS. To avoid potential problems associated with including an explanatory factor (family) that explains much of the phylogenetic tree topology, we removed the phylogenetic correlation among the families for this analysis. To do this, the deeper branches of the phylogeny—those below the family level—were collapsed into a polytomy while retaining the ultrametric nature of the tree (Figure S3b,d; see also Figure S4b,d). Both neonate larval mass and family were used as explanatory variables, and the Brownian motion phylogenetic correlation structure (function 'corBrownian'; Paradis et al., 2004) was specified for residuals when analysing family-level variation. The use of Brownian motion correlation structure was justified as Pagel's λ was essentially one (see Section 3) and 'corPagel' does not work well with a polytomous tree. Here, there was no need to model heteroscedasticity similarly as above ($\Delta\text{AICc} = 0.713$ in favour of the model not including a variance function).

We analysed variation in GDS similarly as explained above for RMIS, except that peak larval mass (ln-transformed) was used as an explanatory variable in the models instead of neonate larval mass. This was to test whether GDS depends on the final body size of a species, with peak larval mass being a good index of species-specific body size. The PGLS models for GDS were not heteroscedastic, so no variance functions were added to the models. For consistency, we tested family-level variation similarly as for RMIS (see Figure S3 for the phylogenetic trees used in the analyses), although investigation of the GD estimates (Figure S6) did not hint at such variation. Finally,

we also tested whether GDS values differ from zero by fitting an intercept-only PGLS model (Pagel's λ correlation structure) to GDS data. Phenotypic data used in the analyses are archived in the Dryad Digital Repository (<https://doi.org/10.5061/dryad.p2ngf1vmz>; Kivelä et al., 2020).

3 | RESULTS

3.1 | Relative mass increment regression

Across studied individuals, RMI varied from 1.33 in instar VII of *O. incerta* (Noctuidae; most *O. incerta* individuals had six instars) to 14.1 in instar I of *Orthosia gothica* (Noctuidae), with an overall median of 4.42. Across species, RMIS, that is the scaling exponent of RMI to body size (i.e. regression slope of $\ln[\text{RMI}]$ on $\ln[\text{instar-specific initial mass}]$), varied from -0.213 in *Endromis versicolora* (the only species from the Endromidae family in our sample) to 0.131 in *Laotloe populi* (Sphingidae; Table S3). RMIS was not affected by the thermal regime of larval rearing, except that the RMIS values were less negative for larvae under the highest temperature (24°C) than the lowest (16°C) temperature (Table 2).

RMIS was predominantly negative (i.e. RMI decreased across instars) in Drepanidae, Endromidae, Erebidae, Geometridae, Noctuidae and Pieridae independently of whether final larval instar was included in RMIS derivation or not (Table S3; see also Figure S7). In Sphingidae, RMIS was positive, and in the studied species of Notodontidae and Nymphalidae, scaling exponents did not differ from zero (Table S3). In most species with negative RMIS, it was in general slightly more negative when final instar was excluded from RMIS derivation (Table S3), implying that the final instar somewhat deviates from the across-instar decrease pattern in RMI. Overall, isometric change in RMIs can be ruled out in most of the studied species due to non-zero RMIS values.

When using neonate larval mass as a predictor for RMIS, there was a strong phylogenetic signal, Pagel's λ being 0.994 (95% CI: $0.893, 1.09$). Neonate larval mass did not explain variation in RMIS (coefficient for $\ln[\text{neonate mass}] = -0.000128$, $SE = 0.00776$, $t = -0.0165$, $p = 0.99$; Figure 2). Excluding the deviating *Endromis versicolora* (Figure 2) did not change this conclusion (coefficient for $\ln[\text{neonate mass}] = 0.00564$, $SE = 0.00819$, $t = 0.689$, $p = 0.50$). There was, however, variation in RMIS among families (Table 3). RMIS was significantly negative in the reference family Endromidae, which was represented by a single species (*E. versicolora*) in our sample. In Notodontidae and Sphingidae, RMIS deviated significantly from the value in Endromidae, with values being positive in both Notodontidae and Sphingidae (Table 3). RMIS values in the rest of the families did not differ significantly from the value in Endromidae (Table 3; see also Figure S5). Removal of the final larval instar from the analysis did not change the results greatly, except that RMIS values in Notodontidae no longer remained positive and RMIS values in Nymphalidae became positive (Appendix B in Supporting Information).

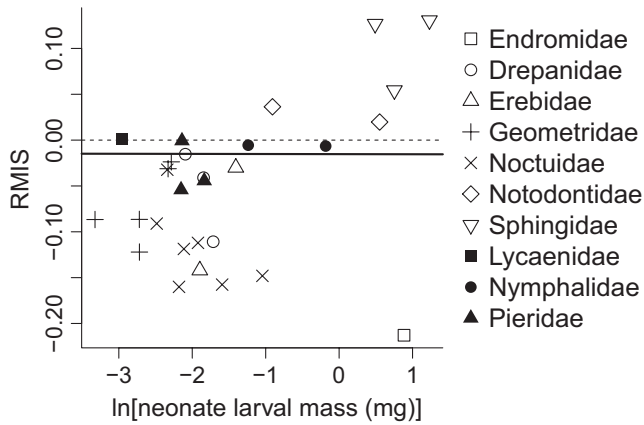


FIGURE 2 Relative mass increment slope (RMIS; i.e. scaling exponent of relative instar-specific mass increment, RMI, to body size) in relation to neonate larval mass (ln-transformed). The horizontal dashed line is the reference line at zero. Negative RMIS values mean a decreasing instar-specific relative mass increments across instars, whereas positive values mean the opposite. The unbroken line is a regression line derived from a phylogenetic generalized least squares model taking the phylogenetic dependency of species into account

TABLE 3 Parameter estimates of a phylogenetic generalized least squares model explaining variation in ontogenetic change in instar-specific relative mass increments (RMIS) among families. The phylogenetic tree used in this analysis was modified so that among-family correlations were removed, resulting in a polytomy of family lineages (see text and Figure S3 for full details) to avoid problems due to the inclusion of the 'family' factor that partially explains the topology of the phylogenetic tree in the model

Parameter	Estimate	SE	t Value	p Value
Intercept (Endromidae)	-0.197	0.0767	-2.566	0.019
ln(neonate mass)	-0.0181	0.0189	-0.959	0.35
Drepanidae	0.0998	0.109	0.913	0.37
Erebidae	0.0809	0.110	0.735	0.47
Geometridae	0.0749	0.116	0.646	0.53
Lycaenidae	0.144	0.128	1.12	0.28
Noctuidae	0.0538	0.111	0.485	0.63
Notodontidae	0.222	0.101	2.20	0.041
Nymphalidae	0.178	0.108	1.64	0.12
Pieridae	0.133	0.113	1.17	0.26
Sphingidae	0.306	0.0989	3.10	0.0062

3.2 | Growth deceleration regression

Individual-specific GD values varied from 0.347 in instar I of *Paradarisa consonaria* (Geometridae) to 5.52 in instar III of *Pararge aegeria* (Nymphalidae), with an overall median of 1.23. Across species, GDS, that is the scaling exponent of GD to body size (i.e. regression slope of ln[GD] on ln[instar-specific peak mass]), varied from -0.00315 in *Endromis versicolora* (Endromidae) to 0.175 in

Pararge aegeria (Nymphalidae; Table S4). Note that negative values of GDS mean a decreasing GD across instars. There was some effect of thermal regime of larval rearing on GDS; GDS values were more positive at 18°C than at the reference temperature of 16°C, with GDS values being positive at 16°C (Table 2).

When using peak larval mass as a predictor for GDS, there was some phylogenetic signal, Pagel's λ being 0.450 (-0.0725, 0.972). There was no statistical evidence of an association between GDS and ln(peak larval mass) (coefficient for ln[peak larval mass] = -0.00464, SE = 0.00539, $t = -0.861$, $p = 0.40$). The independence of GDS from ln(peak larval mass) means that the ontogenetic change in GD across instars is not affected by final body size of the larva in an interspecific comparison. Exclusion of the final larval instar from the analysis did not change these patterns (Appendix B).

There was no evidence of biologically meaningful GDS variation among families (Table S5). Yet, the moderate phylogenetic signal in analysis of GDS in relation to peak larval mass (see PGLS results above) appears not to be a consequence of the data simply being noisy. This is because GDS varied among species when analysing data consisting of individual-specific GDS values with a linear model in which only species was set as a factor ($F_{29,393} = 3.05$, $p < 0.0001$, $R^2 = 0.18$). As further evidence of GDS being a biologically meaningful index, GDS values were consistently positive, the only exception being *Endromis versicolora* (Figure 3; Table S4; see also Figure S8). Across species, GDS values differed statistically from zero as the intercept-only PGLS model estimated GDS to be significantly positive (intercept = 0.0715, SE = 0.0112, $t = 6.40$, $p < 0.0001$), and the confidence intervals of most species-specific GDS estimates did not encompass zero (Table S4). Positive GDS values mean that instar-specific GD becomes stronger with increasing body size during ontogeny when comparing different instars within a species. Because isometric scaling of GD to body size would mean GDS = 0, the observed scaling

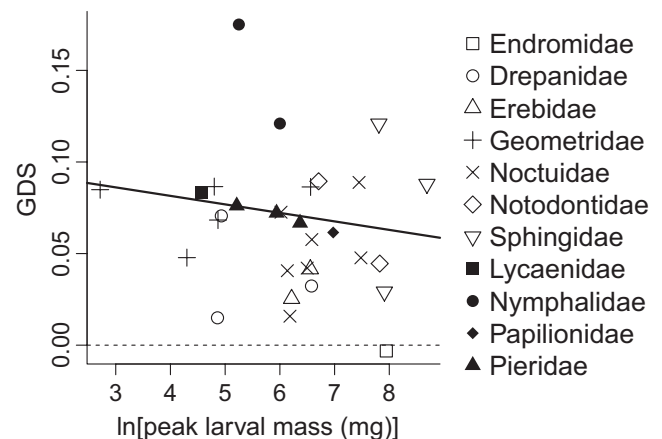


FIGURE 3 Growth deceleration slope (GDS; i.e. scaling exponent of end-of-instar growth deceleration, GD, to body size) in relation to peak larval mass (ln-transformed). The horizontal dashed line is the reference line at zero. Negative GDS values mean that end-of-instar GD becomes weaker across instars, whereas positive values mean the opposite. The unbroken line is a regression line derived from a phylogenetic generalized least squares model taking the phylogenetic dependency of species into account

(Figure 3; Table S4) appears hyperallometric. When the final larval instar was excluded from the analysis, GDS values remained significantly positive in an intercept-only PGLS model (Appendix B), yet the species-specific GDS values tended to decrease (Table S4).

4 | DISCUSSION

Our comparative analysis of larval growth trajectories in Lepidoptera reveals both evolving and constrained growth trajectory characteristics. We focused on relative instar-specific mass increments (RMIs) and end-of-instar growth deceleration (GD), both of which typically changed across instars independently of thermal regime. Across-instar change in RMI (measured as RMI slope across instars, i.e. RMIS; see above) varies among taxonomic families, indicating that the mechanism determining RMIS is flexible enough to change at the macroevolutionary scale, yet it appears constrained within families. Alternatively, the within-family conservativeness of RMIS arises because species belonging to the same family experience similar selection pressures, but this explanation seems unlikely due to the ecological diversity and consequently divergent selection pressures between species within lepidopteran families. In most of the studied families, RMIS was negative, which means that RMI decreases across instars. The opposite pattern, increasing RMI across instars (i.e. positive RMIS), was found in Sphingidae. Conversely, ontogenetic change in GD, measured as GD slope across instars (i.e. GDS; see above), was very similar in all studied families. GDS was generally positive and independent of body size, which means that GD becomes stronger with increasing body size across instars during ontogeny, and this ontogenetic change was similar across species with different body sizes. It is also worth noting that the allometric exponent of GD (i.e. GDS) varied less among species (range: -0.00315 , 0.175 ; $SD = 0.0363$) than the allometric exponent of RMI (i.e. RMIS; range: -0.213 , 0.131 ; $SD = 0.0822$), suggesting stronger constraints on ontogenetic change in GD. Taken together, the results indicate that larval growth is not isometric as both RMIS and GDS were generally non-zero, while isometry, implied by Dyar's Rule, would have produced RMIS and GDS equal to zero.

4.1 | Constrained evolution and plastic variation in growth trajectories

The evolution of both RMIS and GDS appears constrained. There is variation in RMIS among taxonomic families and, besides that, subtle variation in the way RMI changes across instars in families with negative RMIS, as indicated by an increasing RMI in the last instar in Drepanidae and Geometridae. Ontogenetic change in RMI is consistent within families, suggesting that either some physiological or developmental constraints slow down within-family evolution (see Roff & Fairbairn, 2007) or that species belonging to the same family experience very similar selection pressures on RMIS. On the other hand, the low variance in GDS among family lineages

suggests that GD is constrained by fundamental developmental or physiological mechanisms so that only a subset of theoretically possible phenotypes can be attained (Roff & Fairbairn, 2007). A shared mechanistic basis of the trait would make it evolutionarily conservative across taxa (see Schwenk & Wagner, 2004; Tammaru et al., 2010, 2015).

Phenotypic plasticity of growth and development (e.g. Esperk et al., 2013; Frazier, Woods, & Harrison, 2001; Gotthard, 2008; Greenberg & Ar, 1996; Välimäki, Kivelä, Mäenpää, & Tammaru, 2013) affects the instar-level characteristics investigated in this study (Grunert et al., 2015; Kivelä et al., 2018; Tammaru et al., 2015). We pooled data from several larval rearing experiments where the rearing conditions were not identical (Table 1), so natural variation in RMI and GD values due to phenotypic plasticity is included in the data. Nevertheless, we focused on the ontogenetic change of RMI and GD across instars (i.e. RMIS and GDS) rather than the instar-specific trait values as such. This across-instar change appears quite insensitive to environmental conditions, as indicated by only a few statistically significant temperature effects on RMIS and GDS (Table 2) in the subset of species for which temperature was systematically manipulated. Consequently, our results are not specific to a single rearing temperature, but are more general and robust.

4.2 | Potential mechanisms underlying the results

Although several mechanisms have been proposed to explain the need to moult for maintaining a high growth rate, there is limited support for many of them. Out of the ultimate hypotheses for moulting, the role that the potentially hypoallometric growth of the midgut has remains speculative with insufficient data (Callier & Nijhout, 2012; Esperk & Tammaru, 2004; Grunert et al., 2015). The size of feeding structures (e.g. mandibles) does not explain growth rate in lepidopteran larvae, indicating that food acquisition rate does not constrain growth (Esperk & Tammaru, 2004). In fact, absolute growth rate increases within an instar despite constant mandible size, and moulting to the next instar does not result in such a growth benefit as would be expected if food acquisition rate limited growth (Esperk & Tammaru, 2004); therefore, the need to renew feeding structures is an unlikely reason for moulting. Moreover, a restricted capacity for extending (i.e. unfolding) the cuticle (Bennet-Clark, 1963) seems to be an unlikely trigger for moulting because juvenile-hormone-treated final-instar *Bombyx mori* and *Manduca sexta* larvae grow unnaturally large during the instar (see Kamimura & Kiuchi, 1998; Nijhout et al., 2006), suggesting that normal growth does not take cuticle expansion capacity close to the limit.

Recently, most attention in moulting physiology has been paid to the oxygen-dependent induction of moulting (ODIM) hypothesis, stating that compromised oxygen supply to growing tissues induces moulting (Callier & Nijhout, 2011; Callier et al., 2013; Frazier et al., 2001; Greenberg & Ar, 1996; Greenlee & Harrison, 2004, 2005; Kivelä, Friberg, et al., 2016; Kivelä, Lehmann, & Gotthard, 2016; Kivelä et al., 2018). The underlying reasoning is based on a

temporal mismatch between an increase in oxygen demand (i.e. tissue growth) and an increase in the oxygen supply capacity of the respiratory system (i.e. volume of the tracheal system). This mismatch arises because the tracheal system principally grows at moults (Lundquist, Kittilson, Ahsan, & Greenlee, 2018; but see Helm & Davidowitz, 2013), whereas tissue mass increases between the moults. Consequently, moulting would ultimately be necessary to build a larger respiratory system before oxygen deficiency becomes too severe. There is indirect (Callier & Nijhout, 2011; Greenlee & Harrison, 2004, 2005; Kivelä, Friberg, et al., 2016; Kivelä, Lehmann, et al., 2016; Lundquist et al., 2018) and direct experimental support for the ODIM hypothesis (Callier & Nijhout, 2011; Callier et al., 2013; Frazier et al., 2001; Kivelä et al., 2018), but existing data are not consistent with the hypothesis in every respect.

The ODIM mechanism would shape the growth trajectory and predicts decreasing RMI across instars, which should become pronounced in the last instar(s) (Kivelä, Friberg, et al., 2016). Within the framework of the ODIM hypothesis, we might also predict a positive GDS. This is because GD should be proportional to the mass of tissues that are short of oxygen at the end of an instar, and the mass of oxygen-deficient tissue will increase with increasing total body size across instars. However, there is no empirical evidence that oxygen limitation would become stronger in larger instars (Lundquist et al., 2018; see also Greenlee & Harrison, 2005). Finally, Callier and Nijhout (2014) hypothesized that compromised availability of metabolic intermediates that act as precursors for growth may result in GD, but it remains unclear how this hypothesized mechanism would shape growth trajectories. Hence, the prediction concerning GD remains vague and may be based on too simplistic assumptions.

The present results were consistent with predictions of the ODIM hypothesis in many respects. RMIS was negative in 8 out of 10 families investigated (Table 3; Figure 2) and GDS was positive in all families except Endromidae (Figure 3; Tables S4 and S5). However, RMI increased in the last instar despite overall negative RMIS in Drepanidae and Geometridae (Figures S5 and S7), contradicting the prediction of the ODIM hypothesis. In the Sphingidae, RMIS was positive, which also contradicts the prediction. There are two potential explanations that would reconcile the deviating RMI results within the ODIM framework: hyperallometric tracheal growth across instars and within-instar tracheal growth. Hyperallometric tracheal growth would increasingly postpone the point at which oxygen demand meets supply across instars, resulting in an across-instar increase in RMI. There is a paucity of data on across-instar tracheal growth, but it appears to be isometric in *Manduca sexta* (Callier & Nijhout, 2011; Lundquist et al., 2018). Within-instar tracheal growth would similarly postpone the point at which oxygen demand surpasses supply, and would thus allow a larva to grow more during the instar. Interestingly, in the sphingid *M. sexta*, tracheal size increases within the final instar (Callier & Nijhout, 2011; Helm & Davidowitz, 2013) but not within earlier instars (Callier & Nijhout, 2011; Lundquist et al., 2018), which

could partially explain the presently observed positive RMIS in Sphingidae. Whether the same mechanism could also explain the last-instar increase in RMI in Drepanidae and Geometridae remains unknown. Comparative data on within- and across-instar tracheal growth would be needed for a rigorous assessment of the ODIM hypothesis and mechanisms underlying the observed patterns.

If the balance between oxygen supply and demand has a role in moult induction, then we also need to consider potential cutaneous respiration (see Chapman, 1998) in very small larvae. This is because small larvae have a high surface area to volume ratio, potentially facilitating efficient gas exchange through the cuticle, which would allow more growth within an instar than would be expected considering the tracheal system alone. There is some indirect evidence that cutaneous respiration may occur in first-instar larvae in some species (Kivelä, Friberg, et al., 2016). The growth benefit attainable via cutaneous respiration should decrease rapidly with increasing body size and is expected to be found only in the very first instar(s) in species with very small neonate larvae. A high RMI in the first instar in relation to the subsequent instars and negative RMIS in Noctuidae, Drepanidae, Endromidae and Geometridae (Table 3; Figure S5) are consistent with a prediction based on the cutaneous respiration hypothesis. However, *Endromis versicolora* (the only studied endromid species) has very large neonate larvae, suggesting that something else other than cutaneous respiration is responsible for the steep decrease in RMIs across instars in this species. Also, the neonate larvae of the sphingids, *Cerura vinula* (Notodontidae) and *Pararge xiphioides* (Nymphalidae) are so large that it is unlikely that they would get a significant growth benefit from cutaneous respiration and, consistently, growth trajectories of these species do not show signs of cutaneous respiration (Figure S7). Our results thus suggest cutaneous respiration in very small larvae, but rigorous physiological studies are needed to demonstrate it.

5 | CONCLUSIONS

Evolutionary life-history studies cannot ignore developmental and physiological mechanisms that shape growth trajectories because these mechanisms form the proximate basis of traits such as age and size at maturity. Research on the model organisms *M. sexta* and *Drosophila melanogaster* has highlighted the evolutionary significance of some proximate mechanisms that operate during the final larval instar in insects (Callier & Nijhout, 2013; Davidowitz et al., 2016; Nijhout et al., 2006, 2010, 2014; Shingleton, 2011). Our work adds to this by showing how comparisons across instars and species can contribute to the understanding of the constraints on the evolution of age and size at maturity. We also demonstrate that there is some variation in growth patterns among evolutionary lineages, which means that caution is required when generalizing results obtained in model organisms.

Despite ubiquitous phenotypic plasticity (e.g. Esperk et al., 2013; Frazier et al., 2001; Gotthard, 2008; Greenberg & Ar, 1996; Tammaru et al., 2015; Välimäki et al., 2013) and within-species genetic variation (e.g. Blanckenhorn & Demont, 2004; Kivelä, Välimäki, Carrasco, Mäenpää, & Oksanen, 2011; Välimäki et al., 2013) in growth trajectories, the possible directions of plasticity and evolution appear to be limited by conservative developmental and physiological mechanisms (Tammaru et al., 2010, 2015; this study). To fully explain and predict plastic and evolutionary variation in growth trajectories, mechanisms generating constraints should be considered. Hence, our results suggest that the classical demographic optimality approach of life-history theory—with age-specific fecundity and mortality depending on trait values (Roff, 2002; Stearns, 1992)—should be supplemented by incorporating developmental and physiological mechanisms into analysis.

ACKNOWLEDGEMENTS

We thank Jon Harrison and three anonymous reviewers for constructive comments on an earlier version of the manuscript. We are grateful to Niko Johansson, Britta Kalgan, Urmas Lanto, Merili Martverk, Laura Tammiste, Alma Tiwe, Beatrice Svensson, Sonja Viinamäki and Panu Välimäki for their help in measuring larval growth trajectories and data handling. Erki Öunap kindly provided samples for the phylogenetic analyses, and Hannele Parkkinen helped in DNA extraction and sequencing. We are also grateful to Vlad Dinca for his help in the derivation of the phylogenetic tree of the study species and to Ants Kaasik for statistical advice. This study was financed by the Finnish Cultural Foundation (S.M.K.), the Emil Aaltonen Foundation (S.M.K.), the Estonian Research Council (PUT1474 to S.M.K.), the international fellowship program at Stockholm University (S.M.K.), Academy of Finland (grant nos. 314833 and 319898 to S.M.K., and grant no. 277984 to M.M.), institutional research funding IUT (IUT20-33) from the Estonian Ministry of Education and Research (R.B.D., D.V., T.E. and T.T.), the Bolin Centre for Climate Research at Stockholm University (K.G.) and the Swedish Research Council (grant VR 2017-04500 to K.G.).

AUTHORS' CONTRIBUTIONS

S.M.K., K.G. and T.T. conceived the initial idea of the study and designed the experiments; S.M.K., T.E., K.G. and D.V. ran the experiments; M.M. organized DNA sequencing, aligned and edited the sequences, and derived the phylogeny; S.M.K., R.B.D. and T.T. ran statistical analyses. All authors contributed to writing of the manuscript and gave final approval for publication.

DATA AVAILABILITY STATEMENT

Phenotypic data deposited in the Dryad Digital Repository <http://doi.org/10.5061/dryad.p2ngf1vmz> (Kivelä et al., 2020). DNA sequence data archived in GenBank (accession numbers given in Table S2).

ORCID

Sami M. Kivelä  <https://orcid.org/0000-0002-6844-9168>

Toomas Tammaru  <https://orcid.org/0000-0002-6892-5910>

REFERENCES

- Bennet-Clark, H. C. (1963). The relation between epicuticular folding and the subsequent size of an insect. *Journal of Insect Physiology*, *9*, 43–46. [https://doi.org/10.1016/0022-1910\(63\)90083-0](https://doi.org/10.1016/0022-1910(63)90083-0)
- Berg, M. B., & Merritt, R. W. (2009). Growth, individual. In V. H. Resh & R. T. Carde (Eds.), *Encyclopedia of insects* (2nd ed., pp. 431–434). London, UK: Academic Press.
- Blackburn, D. G., & Evans, H. E. (1986). Why are there no viviparous birds? *The American Naturalist*, *128*, 165–190. <https://doi.org/10.1086/284552>
- Blanckenhorn, W. U., & Demont, M. (2004). Bergmann and converse Bergmann latitudinal clines in Arthropods: Two ends of a continuum? *Integrative and Comparative Biology*, *44*, 413–424. <https://doi.org/10.1093/icb/44.6.413>
- Callier, V., & Nijhout, H. F. (2011). Control of body size by oxygen supply reveals size-dependent and size-independent mechanisms of molting and metamorphosis. *Proceedings of the National Academy of Sciences of the United States of America*, *108*, 14664–14669. <https://doi.org/10.1073/pnas.1106556108>
- Callier, V., & Nijhout, H. F. (2012). Supply-side constraints are insufficient to explain the ontogenetic scaling of metabolic rate in the Tobacco Hornworm, *Manduca sexta*. *PLoS ONE*, *7*, e45455. <https://doi.org/10.1371/journal.pone.0045455>
- Callier, V., & Nijhout, H. F. (2013). Body size determination in insects: A review and synthesis of size- and brain-dependent and independent mechanisms. *Biological Reviews*, *88*, 944–954. <https://doi.org/10.1111/brv.12033>
- Callier, V., & Nijhout, H. F. (2014). Plasticity of insect body size in response to oxygen: Integrating molecular and physiological mechanisms. *Current Opinion in Insect Science*, *1*, 59–65. <https://doi.org/10.1016/j.cois.2014.05.007>
- Callier, V., Shingleton, A. W., Brent, C. S., Ghosh, S. M., Kim, J., & Harrison, J. F. (2013). The role of reduced oxygen in the developmental physiology of growth and metamorphosis initiation in *Drosophila melanogaster*. *Journal of Experimental Biology*, *216*, 4334–4340. <https://doi.org/10.1242/jeb.093120>
- Chapman, R. F. (1998). *The insects, structure and function* (4th ed.) Cambridge, UK: Cambridge University Press.
- Darriba, D., Taboada, G. L., Doallo, R., & Posada, D. (2012). jModelTest 2: More models, new heuristics and parallel computing. *Nature Methods*, *9*, 772. <https://doi.org/10.1038/nmeth.2109>
- Davidowitz, G., Roff, D., & Nijhout, H. F. (2016). Synergism and antagonism of proximate mechanisms enable and constrain the response to simultaneous selection on body size and development time: An empirical test using experimental evolution. *The American Naturalist*, *188*, 499–520. <https://doi.org/10.1086/688653>
- Drummond, A. J., & Rambaut, A. (2007). BEAST: Bayesian evolutionary analysis by sampling trees. *BMC Evolutionary Biology*, *7*, 214. <https://doi.org/10.1186/1471-2148-7-21>
- Dunbrack, R. L., & Ramsay, M. A. (1989). The evolution of viviparity in amniote vertebrates: Egg retention versus egg size reduction. *The American Naturalist*, *133*, 138–148. <https://doi.org/10.1086/284905>
- Dyar, H. G. (1890). The number of molts of lepidopterous larvae. *Psyche*, *5*, 420–422. <https://doi.org/10.1155/1890/23871>
- Esperk, T., Stefanescu, C., Teder, T., Wiklund, C., Kaasik, A., & Tammaru, T. (2013). Distinguishing between anticipatory and responsive plasticity in a seasonally polyphenic butterfly. *Evolutionary Ecology*, *27*, 315–332. <https://doi.org/10.1007/s10682-012-9598-7>
- Esperk, T., & Tammaru, T. (2004). Does the 'investment principle' model explain molting strategies in lepidopteran larvae? *Physiological Entomology*, *29*, 56–66. <https://doi.org/10.1111/j.1365-3032.2004.0365.x>
- Esperk, T., Tammaru, T., & Nylin, S. (2007). Intraspecific variability in number of larval instars in insects. *Journal of Economic Entomology*, *100*, 627–645.

- [https://doi.org/10.1603/0022-0493\(2007\)100\[627:ivino\]2.0.co;2](https://doi.org/10.1603/0022-0493(2007)100[627:ivino]2.0.co;2)
- Esperk, T., Tammaru, T., Nylin, S., & Teder, T. (2007). Achieving high sexual size dimorphism in insects: Females add instars. *Ecological Entomology*, 32, 243–256. <https://doi.org/10.1111/j.1365-2311.2007.00872.x>
- Flatt, T., & Heyland, A. (Eds.). (2011). *Mechanisms of life history evolution: The genetics and physiology of life history traits and trade-offs*. Oxford, UK: Oxford University Press.
- Frazier, M. R., Woods, H. A., & Harrison, J. F. (2001). Interactive effects of rearing temperature and oxygen on the development of *Drosophila melanogaster*. *Physiological and Biochemical Zoology*, 74, 641–650. <https://doi.org/10.1086/322172>
- Gokhale, R. W., & Shingleton, A. W. (2015). Size control: The developmental physiology of body and organ size regulation. *Wiley Interdisciplinary Reviews: Developmental Biology*, 4, 335–356. <https://doi.org/10.1002/wdev.181>
- Gotthard, K. (2008). Adaptive growth decisions in butterflies. *BioScience*, 58, 222–230. <https://doi.org/10.1641/B580308>
- Gould, S. J., & Lewontin, R. C. (1979). The spandrels of San Marco and the Panglossian paradigm: A critique of the adaptationist programme. *Proceedings of the Royal Society B*, 205, 581–598. <https://doi.org/10.1098/rspb.1979.0086>
- Greenberg, S., & Ar, A. (1996). Effects of chronic hypoxia, normoxia and hyperoxia on larval development in the beetle *Tenebrio molitor*. *Journal of Insect Physiology*, 42, 991–996. [https://doi.org/10.1016/S0022-1910\(96\)00071-6](https://doi.org/10.1016/S0022-1910(96)00071-6)
- Greenlee, K. J., & Harrison, J. F. (2004). Development of respiratory function in the American locust *Schistocerca americana*: II. Within-instar effects. *Journal of Experimental Biology*, 207, 509–517. <https://doi.org/10.1242/jeb.00766>
- Greenlee, K. J., & Harrison, J. F. (2005). Respiratory changes throughout ontogeny in the tobacco hornworm caterpillar, *Manduca sexta*. *Journal of Experimental Biology*, 208, 1385–1392. <https://doi.org/10.1242/jeb.01521>
- Grunert, L. W., Clarke, J. W., Ahuja, C., Eswaran, H., & Nijhout, H. F. (2015). A quantitative analysis of growth and size regulation in *Manduca sexta*: The physiological basis of variation in size and age at metamorphosis. *PLoS ONE*, 10, e0127988. <https://doi.org/10.1371/journal.pone.0127988>
- Hall, T. (1999). BioEdit: A user-friendly biological sequence alignment editor and analysis program for Windows 95/98/NT. *Nucleic Acids Symposium Series*, 41, 95–98.
- Heikkilä, M., Kaila, L., Mutanen, M., Pena, C., & Wahlberg, N. (2012). Cretaceous origin and repeated Tertiary diversification of the redefined butterflies. *Proceedings of the Royal Society B*, 279, 1093–1099. <https://doi.org/10.1098/rspb.2011.1430>
- Helm, B. R., & Davidowitz, G. (2013). Mass and volume growth of an insect tracheal system within a single instar. *Journal of Experimental Biology*, 216, 4703–4711. <https://doi.org/10.1242/jeb.080648>
- Hironaka, K., & Morishita, Y. (2017). Adaptive significance of critical weight for metamorphosis in holometabolous insects. *Journal of Theoretical Biology*, 417, 68–83. <https://doi.org/10.1016/j.jtbi.2017.01.014>
- Hutchinson, J. M. C., McNamara, J. M., Houston, A. I., & Vollrath, F. (1997). Dyar's Rule and the Investment Principle: Optimal moulting strategies if feeding rate is size-dependent and growth is discontinuous. *Philosophical Transactions of the Royal Society of London B*, 352, 113–138. <https://doi.org/10.1098/rstb.1997.0007>
- Kamimura, M., & Kiuchi, M. (1998). Effects of juvenile hormone analog, fenoxycarb, on 5th stadium larvae of the silkworm, *Bombyx mori* (Lepidoptera: Bombycidae). *Applied Entomology and Zoology*, 33, 333–338. <https://doi.org/10.1303/aez.33.333>
- Kilmer, J. T., & Rodriguez, R. L. (2017). Ordinary least squares regression is indicated for studies of allometry. *Journal of Evolutionary Biology*, 30, 4–12. <https://doi.org/10.1111/jeb.12986>
- Kivelä, S. M., Davis, R. B., Esperk, T., Gotthard, K., Mutanen, M., Valdma, D., & Tammaru, T. (2020). Data from: Comparative analysis of larval growth in Lepidoptera reveals instar-level constraints. *Dryad Digital Repository*, <https://doi.org/10.5061/dryad.p2ngf1vmz>
- Kivelä, S. M., Friberg, M., Wiklund, C., Leimar, O., & Gotthard, K. (2015). Data from: Towards a mechanistic understanding of insect life history evolution: A model based on oxygen-dependent induction of molting successfully explains molting sizes. *Dryad Digital Repository*, <https://doi.org/10.5061/dryad.5h3k3>
- Kivelä, S. M., Friberg, M., Wiklund, C., Leimar, O., & Gotthard, K. (2016). Towards a mechanistic understanding of insect life history evolution: Oxygen-dependent induction of molting explains molting sizes. *Biological Journal of the Linnean Society*, 117, 586–600. <https://doi.org/10.1111/bij.12689>
- Kivelä, S. M., Lehmann, P., & Gotthard, K. (2016). Do respiratory limitations affect metabolism of insect larvae before molting? An empirical test at the individual level. *Journal of Experimental Biology*, 219, 3061–3071. <https://doi.org/10.1242/jeb.140442>
- Kivelä, S. M., Välimäki, P., Carrasco, D., Mäenpää, M. I., & Oksanen, J. (2011). Latitudinal insect body size clines revisited: A critical evaluation of the saw-tooth model. *Journal of Animal Ecology*, 80, 1184–1195. <https://doi.org/10.1111/j.1365-2656.2011.01864.x>
- Kivelä, S. M., Viinämäki, S., Keret, N., Gotthard, K., Hohtola, E., & Välimäki, P. (2018). Elucidating mechanisms for insect body size: Partial support for the oxygen-dependent induction of molting hypothesis. *Journal of Experimental Biology*, 221, jeb166157. <https://doi.org/10.1242/jeb.166157>
- Kühnel, S., Brückner, A., Schmelzle, S., Heethoff, M., & Blüthgen, N. (2017). Surface area-volume ratios in insects. *Insect Science*, 24, 829–841. <https://doi.org/10.1111/1744-7917.12362>
- Leimar, O. (1996). Life history plasticity: Influence of photoperiod on growth and development in the common blue butterfly. *Oikos*, 76, 228–234. <https://doi.org/10.2307/3546194>
- Lundquist, T. A., Kittilson, J. D., Ahsan, R., & Greenlee, K. J. (2018). The effect of within-instar development on tracheal diameter and hypoxia-inducible factors α and β in the tobacco hornworm, *Manduca sexta*. *Journal of Insect Physiology*, 106, 199–208. <https://doi.org/10.1016/j.jinsphys.2017.12.001>
- Meister, H., Hämäläinen, H. R., Valdma, D., Martverk, M., & Tammaru, T. (2018). How to become larger: Ontogenetic basis of among-population size differences in a moth. *Entomologia Experimentalis et Applicata*, 166, 4–16. <https://doi.org/10.1111/eea.12634>
- Miller, M. A., Pfeiffer, W., & Schwartz, T. (2010). Creating the CIPRES Science Gateway for inference of large phylogenetic trees. *Proceedings of the Gateway Computing Environments Workshop (GCE)*. New Orleans, LA, pp. 1–8. <https://doi.org/10.1109/GCE.2010.5676129>
- Mutanen, M., Wahlberg, N., & Kaila, L. (2010). Comprehensive gene and taxon coverage elucidates patterns of radiation of moths and butterflies. *Proceedings of the Royal Society B*, 277, 2839–2848. <https://doi.org/10.1098/rspb.2010.0392>
- Nijhout, H. F., Davidowitz, G., & Roff, D. A. (2006). A quantitative analysis of the mechanism that controls body size in *Manduca sexta*. *Journal of Biology*, 5, 16. <https://doi.org/10.1186/jbiol43>
- Nijhout, H. F., Riddiford, L. M., Mirth, C., Shingleton, A. W., Suzuki, Y., & Callier, V. (2014). The developmental control of size in insects. *Wiley Interdisciplinary Reviews: Developmental Biology*, 3, 113–134. <https://doi.org/10.1002/wdev.124>
- Nijhout, H. F., Roff, D. A., & Davidowitz, G. (2010). Conflicting processes in the evolution of body size and development time. *Philosophical Transactions of the Royal Society B: Biological Sciences*, 365, 567–575. <https://doi.org/10.1098/rstb.2009.0249>
- Paradis, E., Claude, J., & Strimmer, K. (2004). APE: Analyses of phylogenetics and evolution in R language. *Bioinformatics*, 20, 289–290. <https://doi.org/10.1093/bioinformatics/btg412>

- Pinheiro, J., Bates, D., DebRoy, S., Sarkar, D., & R Core Team. (2017). nlme: Linear and nonlinear mixed effects models. R package version 3.1-131. Retrieved from <https://CRAN.R-project.org/package=nlme>
- R Core Team. (2017). *R: A language and environment for statistical computing*. Vienna, Austria: R Foundation for Statistical Computing. Retrieved from <https://www.R-project.org/>
- Rambaut, A., Suchard, M. A., Xie, D., & Drummond, A. J. (2014). Tracer v1.6. Retrieved from <http://beast.bio.ed.ac.uk/Tracer>
- Roff, D. A. (2002). *Life history evolution*. Sunderland, MA: Sinauer Associates.
- Roff, D. A., & Fairbairn, D. J. (2007). The evolution of trade-offs: Where are we? *Journal of Evolutionary Biology*, 20, 433–447. <https://doi.org/10.1111/j.1420-9101.2006.01255.x>
- Schwenk, K., & Wagner, G. P. (2004). The relativism of constraints on phenotypic evolution. In M. Pigliucci & K. Preston (Eds.), *Phenotypic integration: Studying the ecology and evolution of complex phenotypes* (pp. 390–408). Oxford, UK: Oxford University Press.
- Shingleton, A. W. (2011). Evolution and the regulation of growth and body size. In T. Flatt & A. Heyland (Eds.), *Mechanisms of life history evolution: The genetics and physiology of life history traits and trade-offs* (pp. 43–55). Oxford, UK: Oxford University Press. <https://doi.org/10.1093/acprof:oso/9780199568765.003.0004>
- Sihvonen, P., Mutanen, M., Kaila, L., Brehm, G., Hausmann, A., & Staude, H. S. (2011). Comprehensive molecular sampling yields a robust phylogeny for geometrid moths (Lepidoptera: Geometridae). *PLoS ONE*, 6, e20356. <https://doi.org/10.1371/journal.pone.0020356>
- Stearns, S. C. (1992). *The evolution of life histories*. Oxford, UK: Oxford University Press.
- Tammaru, T. (1998). Determination of adult size in a folivorous moth: Constraints at instar level? *Ecological Entomology*, 23, 80–89. <https://doi.org/10.1046/j.1365-2311.1998.00106.x>
- Tammaru, T., & Esperk, T. (2007). Growth allometry of immature insects: Larvae do not grow exponentially. *Functional Ecology*, 21, 1099–1105. <https://doi.org/10.1111/j.1365-2435.2007.01319.x>
- Tammaru, T., Esperk, T., Ivanov, V., & Teder, T. (2010). Proximate sources of sexual size dimorphism in insects: Locating constraints on larval growth schedules. *Evolutionary Ecology*, 24, 161–175. <https://doi.org/10.1007/s10682-009-9297-1>
- Tammaru, T., Vellau, H., Esperk, T., & Teder, T. (2015). Searching for constraints by cross-species comparison: Reaction norms for age and size at maturity in insects. *Biological Journal of the Linnean Society*, 114, 296–307. <https://doi.org/10.1111/bij.12417>
- Välimäki, P., Kivelä, S. M., Mäenpää, M. I., & Tammaru, T. (2013). Latitudinal clines in alternative life histories in a geometrid moth. *Journal of Evolutionary Biology*, 26, 118–129. <https://doi.org/10.1111/jeb.12033>
- Wahlberg, N., & Wheat, C. W. (2008). Genomic outposts serve the phylogenomic pioneers: Designing novel nuclear markers for genomic DNA extractions of Lepidoptera. *Systematic Biology*, 57, 231–242. <https://doi.org/10.1080/10635150802033006>
- Zahiri, R., Kitching, I. J., Lafontaine, J. D., Mutanen, M., Kaila, L., Holloway, J. D., & Wahlberg, N. (2010). A new molecular phylogeny offers hope for a stable family-level classification of the Noctuoidea (Lepidoptera). *Zoologica Scripta*, 40, 158–173. <https://doi.org/10.1111/j.1463-6409.2010.00459.x>

SUPPORTING INFORMATION

Additional supporting information may be found online in the Supporting Information section.

How to cite this article: Kivelä SM, Davis RB, Esperk T, et al. Comparative analysis of larval growth in Lepidoptera reveals instar-level constraints. *Funct Ecol*. 2020;34:1391–1403. <https://doi.org/10.1111/1365-2435.13556>